Article

Estimation of evapotranspiration and categorized maps of climate parameters applicable for civil and architectural designs

Mohammad Valipour

Received: date; Accepted: date; Published: date
Academic Editor: name

Young Researchers and Elite Club, Kermanshah Branch, Islamic Azad University, Kermanshah, Iran
vali-pour@hotmail.com

Abstract: This study aims to estimate the potential evapotranspiration as well as to extract categorized maps of climate parameters that are applicable for civil and architectural design . The results showed that the Albrecht model estimates the potential evapotranspiration better than other models in the most provinces of Iran. The best values of R^2 were 0.9854 and 0.9826 for the Brockamp-Wenner and Albrecht models in Bushehr (BU) and TE provinces, respectively. Finally, a list of the best performance of each model has been presented. The best weather conditions (not only for Iran but also for all countries) to use mass transfer-based equations are 23.6-24.6 MJ/m^2/day, 12-26 ℃, 18-30 ℃, 5-21 ℃, and 2.50-3.25 m.s^{-1} for solar radiation, mean, maximum, and minimum temperature, and wind speed, respectively. The results are also useful for selecting the best model when researchers must apply humidity-based models on the basis of available data. In addition, the designed maps and categories are applicable for considering the role of climatic parameters in architectural evaluations over Iran.

Keywords: architecture; humidity; Iran; linear regression; mass transfer; prevailing wind

PACS: J0101

1. Introduction

The best estimations of actual evapotranspiration are obtained by using lysimeter or imaging techniques, the costs of which are very high [1-7]. Thus, the FAO Penman-Monteith model [8] has become one modelling approach to estimate the potential evapotranspiration [9-14]. Although, the FAO Penman-Monteith (FPM) has been applied in various regions of the world [15-24], its application requires many parameters which are often difficult to obtain. To this end, experimental models have been developed for estimation of the potential evapotranspiration using limited data. They include mass transfer, radiation, temperature, and pan evaporation-based models. The mass transfer-based model is one of the most widely used models to estimate potential evapotranspiration. The common mass transfer-based models include Papadakis, Rohwer, Dalton, Ivanov, Meyer, Trabert, and WMO [25-35].

In the previous studies, one or more of the mass transfer-based models have been compared with temperature, radiation, or pan evaporation-based models and in the most of the cases, other models (temperature, radiation, or pan evaporation-based models) estimated the potential evapotranspiration better than the mass transfer-based models. Because the previous studies focus on specific (humid, arid, semiarid, etc.) weather conditions (that they aren't suitable for applying the mass transfer-based model) and/or didn't consider many methods of mass transfer-based models. Moreover, the results of previous studies are not useable for estimation of the potential evapotranspiration in other regions. Because they were recommended for one or more climatic conditions, but a climatic condition contains a wide range of magnitude of each weather parameter (e.g. temperature, relative humidity, wind speed, solar radiation, etc.) and results of each research (for a region with specific weather variations) is not applicable to other regions without determining specified ranges of each weather parameter even if climatic conditions (e.g. humid, arid, semi-arid, temperate, etc.) are identical for both regions. In addition, the governments cannot schedule for irrigation and agricultural water management when the potential evapotranspiration is estimated for a basin, wetland, watershed, or catchment instead a state or province (different parts of them are located in more than one state or province) and/or number of weather station used is low (increasing uncertainty). Since, this study aims to estimate the potential evapotranspiration for 31 provinces of Iran (considering various weather conditions and useful for long-term and macroeconomic policies of governments) using average data of 181 synoptic stations (decreasing uncertainty) and by 11 mass transfer-based models to determine the best model based on the weather conditions of each province (for which ranges of weather parameters have been determined to use other regions and next researches).

2. Materials and Methods

In this study, weather information (from 1986 to 2005) has been gathered from 181 synoptic stations of 31 provinces in Iran (without data gaps). Table 1 shows the position of each province and number of stations.

Table 1

In each station, average of weather data in years measured has been considered as the value of that weather parameter in each month (e.g. value of relative humidity in July for North Khorasan (NK) is average of 20 data gathered). Finally, average of data in all stations has been considered as the value of that weather parameter in each month for provinces with more than one station (e.g. value of relative humidity in July for KH is average of 20×14=280 data gathered). All of the data mentioned have been used to estimate the potential evapotranspiration using 11 mass transfer-based models and were compared with FPM model to determine the best model based on the weather conditions of each province (Table 2).

Table 2

The best model for each province and the best performance of each model were determined using the coefficient of determination:

$$R^2 = 1 - \frac{\sum \left(ET_{FPM_i} - ET_{m_i}\right)^2}{\sum \left(ET_{FPM_i} - \frac{\sum ET_{FPM_i}}{12}\right)^2} \tag{1}$$

In which, i indicates the month, ETFPM indicates the potential evapotranspiration calculated for FPM model, and ETm indicates the potential evapotranspiration calculated for mass transfer-based models.

Finally, map of the annual average of solar radiation, mean, maximum, and minimum temperature, relative humidity, and wind speed were provided and the best performance of each model based on these values was determined. Furthermore, the map of the best model for each province and the map of the error calculated for each province have been presented.

3. Results and Discussion

3.1. Estimating the potential evapotranspiration for 31 provinces of Iran

Table 3 shows the errors for each model and province.

Table 3

According to the R2-values, each model estimates the potential evapotranspiration for only one or few provinces with very high accuracy. In the other words, preciseness of estimating by mass transfer-based models is very sensitive to variations of the parameters used in each model (Table 2).

3.2. Comparison of the best models for each province

Figure 1 compares the potential evapotranspiration using FPM with values estimated using the best method (based on Table 3) for each province.

Fig. 1

According to Fig. 1 the Brockamp-Wenner for BU (R2=0.9854) yielded the best the potential evapotranspiration as compared to that from the FPM. However, the Albrecht has been introduced as the best model in the most of the provinces (23 provinces). In general, mass transfer-based models are more suitable (R2 more than 0.97) for BU, HO (near the Persian Gulf), SK, KE, SB (south east of Iran) and TE, GI, and ES (south of Iran). However, according to Table 3, variations of the errors (the worst and best R2) for different models are too high in all provinces; e.g. CB (0.839 and 0.9671 for the Penman and Albrecht, respectively), BU (0.8932 and 0.9854 for the Papadakis and Albrecht, respectively), SB (0.8846 and 0.9775 for the Papadakis and WMO, respectively), and HO (0.8083 and 0.9742 for the Ivanov and Albrecht, respectively). These values indicate very different performance of the mass transfer-based models for a specific weather condition in each province. For instance, the Ivanov model estimates the potential evapotranspiration with the least R2 for HO and the greatest R2 for EA than the other models. However, according to Table 2, the Ivanov model is a function of mean temperature and relative humidity, the Papadakis is a function of minimum and maximum temperature and relative humidity, and the other models are a function of mean, minimum, and maximum temperature, relative humidity, and wind speed. In addition, the only difference among the Albrecht, Dalton, Meyer, Rohwer, and WMO models is coefficients used in each model (Table 2) as well as the only difference among the Brockamp-Wenner, Mahringer, and Trabert models is also coefficients used in each model (Table 2). Thus we must use them according to their best weather conditions (with the most accuracy).

3.3. Distinguishing various regions based on weather conditions

The maps of the annual average of the weather parameters have been provided to detect the best conditions (range of weather parameters) that each model estimates the potential evapotranspiration with maximum preciseness (Figs. 2 and 3).

Fig. 2

Fig. 3

Fig. 2 shows the annual average of solar radiation and mean, maximum, and minimum temperature in all 31 provinces of Iran and Fig. 3 shows the annual average of relative humidity and wind speed in all 31 provinces of Iran. As shown, value of solar radiation is more than 25.0 MJ.m-2.day-1 for south of Iran, it is from 24.0 to 25.0 MJ.m-2.day-1 for centre of Iran, and it ranges less than 24.0 MJ.m-2.day-1 for north of Iran. The mean temperature is less than 14 ◎ for north west of Iran, it is more than 24 ◎ near the Persian Gulf, and it is from 14 to 24 ◎ for the other regions (with the exception of NK and CB). The maximum temperature is more than 28.5 ◎ near the Persian Gulf, it is from 25.5 to 27.0 ◎ for desert provinces, it is less than 19.5 ◎ for north west of Iran, and it is from 19.5 to 25.5 ◎ for the other regions. The minimum temperature is more than 17 ◎ near the Persian Gulf, it is less than 7 ◎ for north west of Iran, it is from 11 to 15 near the Caspian Sea, and it is from 7 to 13 ◎ for the other regions (with the exception of CB, NK, KE). The relative humidity is from 65 to 70% near the Persian Gulf (with the exception of KH), it is from 50 to 65% in the north west and north east of Iran (with the exception of AR), it is more than 70% near the Caspian Sea, and it is less than 45% for other regions. The wind speed is from 2.50 to 3.50 m.s-1 for south east of Iran and near the Persian Gulf, and it is from 1.25 to 2.75 m.s-1 for the other regions (with the exception of EA, AR, GO, and CB). The wind speed plays an important role in architectural studies to design buildings and structures with respect to the prevailing wind. For instance, in Qazvin, prevailing wind is a south–eastern wind called Raz or Shareh [45-46]. This wind comes from desert areas of central Iran and is very warm and dry; hence it is reasonable that reduction of the WS due to desertification approaches [47] leads to decreasing impacts of the mentioned climate and consequently reducing the

ETo. Therefore, the WS and may be introduced as the most influencing factors on variations of the ETo in Qazvin.

The mass transfer-based models estimated the potential evapotranspiration in the south (near the Persian Gulf) and south east of Iran (annual relative humidity 65-70% and <35%, respectively) better than other provinces (Fig. 1). Therefore, the provinces of Iran are divided into five categories (at least); (I) the provinces near the Persian Gulf (KH, BU, and HO), (II) the provinces of near the Caspian Sea (GI, MZ, and GO), (III) the provinces of north east of Iran (WA, EA, AR, and ZA), (IV) CB (due to the difference weather conditions than the near provinces), and (V) the other provinces. These categories are useful for future studies over Iran because these four parameters (light, temperature, wind, and humidity) can employ to optimum design in architectural investigations.

3.4. Determining a range of weather parameters for the best models

The maps of annual average of weather parameters (Figs. 2 and 3) are useful not only for the mentioned categories, but also for determining the range of each parameter for which the best preciseness of the mass transfer-based models is obtained (Table 4).

Table 4

According to Table 4, the best performance of the Brockamp-Wenner, Mahringer, Meyer, Trabert, and WMO models is in similar weather conditions (T=24-26 ◎, Tmax=28.5-30.0 ◎, Tmin=19-21 ◎, RH=65-70%, and u=3.00-3.25 m.s-1). However, the precise of them is different (e.g. 0.9783 and 0.9854 for the WMO and Brockamp-Wenner models, respectively). This underlines the important role of selection of the best model for a specified weather conditions. Furthermore, we can see different ranges in the Albrecht, Dalton, Ivanov, Penman, Rohwer, and Papadakis models (Table 4). Therefore, we can use the mass transfer-based models for other regions (in other countries) based on Table 4 with respect to their errors. The best weather conditions to use mass transfer-based equations are 23.6-24.6 MJ/m2/day, 12-26 ◎, 18-30 ◎, 5-21 ◎, and 2.50-3.25 m.s-1 (with the exception of Penman) for solar radiation, mean, maximum, and minimum temperature, and wind speed, respectively. Results are also useful for selecting the best model when researchers must apply temperature-based models on the basis of available data.

3.5. Comparison of the best models with their errors for each province

Figure 4 was plotted to detect the best model for each province versus its error (after calibration).

Fig. 4

First, although the Albrecht model is the most useful model for provinces of Iran (23 provinces), but it is not suitable for 2 of the categories (near the Persian Gulf and north east of Iran) and east of Iran (NK, RK, SK, and SB). This confirms that the categories are reliable and these 2 categories need to more attention due to specific weather conditions. Moreover, the preciseness of the Albrecht model is less than 0.98 in 18 provinces of Iran. It reveals that the Albrecht model is a general model for estimating the potential evapotranspiration (high application and fair preciseness). Thus, we need to other temperature, radiation, and pan evaporation-based models to estimate the potential evapotranspiration in these 18 provinces. For instance, values of solar radiation are more than 25.0 MJ.m-2.day-1 for FA and KB, hence the radiation-based models may be useful for these provinces [48-54]. It reveals that only if we use the mass transfer-based models for suitable (based on Table 4) and specific (based on Figs. 2 and 3) weather conditions, the highest preciseness of estimating will be obtained.

Conflicts of Interest: The authors declare no conflict of interest.

Table 1 Position of all provinces and synoptic stations

Province	Latitude (N)	Longitude (E)	Number of Station
Alborz (AL)	35° 55’	50° 54’	1
Ardabil (AR)	38° 15’	48° 17’	4
Bushehr (BU)	28° 59’	50° 50’	5
Chaharmahal and Bakhtiari (CB)	32° 17’	50° 51’	4
East Azerbaijan (EA)	38° 05’	46° 17’	10
Esfahan (ES)	32° 37’	51° 40’	12
Fars (FA)	29° 32’	52° 36’	9
Ghazvin (GH)	36° 15’	50° 03’	2
Gilan (GI)	37° 15’	49° 36’	4
Gorgan (GO)	36° 51’	54° 16’	3
Hamedan (HA)	34° 52’	48° 32’	4
Hormozgan (HO)	27° 13’	56° 22’	9
Ilam (IL)	33° 38’	46° 26’	3
Kohgiluyeh and Boyer-Ahmad (KB)	30° 50’	51° 41’	1
Kerman (KE)	30° 15’	56° 58’	8
Khuzestan (KH)	31° 20’	48° 40’	14
Kurdistan (KO)	35° 20’	47° 00’	7
Kermanshah (KS)	34° 21’	47° 09’	6
Lorestan (LO)	33° 26’	48° 17’	9

Markazi (MA)	34° 06’	49° 46’	4
Mazandaran (MZ)	36° 33’	53° 00’	7
North Khorasan (NK)	37° 28’	57° 16’	1
Qom (QO)	34° 42’	50° 51’	1
Razavi Khorasan (RK)	36° 16’	59° 38’	12
Sistan and Baluchestan (SB)	29° 28’	60° 05’	8
Semnan (SE)	35° 35’	53° 33’	4
South Khorasan (SK)	32° 52’	59° 12’	3
Tehran (TE)	35° 41’	51° 19’	8
West Azerbaijan (WA)	37° 32’	45° 05’	8
Yazd (YA)	31° 54’	54° 17’	6
Zanjan (ZA)	36° 41’	48° 29’	4

۱۹۳

Table 2 Model used and parameters applied in each model

Model	Reference(s)	Formula	Parameters
FAO Penman-Monteith	Allen et al. [8]	$ET_o = \dfrac{0.408(R_n - G) + \gamma \frac{900}{T+273} u(e_s - e_a)}{\Delta + \gamma(1+0.34u)}$	H,φ,T,T_{min}, T_{max},RH,u,n
Albrecht	Albrecht [25]	$ET_o = (1.005+2.97u)(e_s-e_a)$	T,T_{min}, T_{max},RH,u
Brockamp-Wenner	Brockamp and Wenner [26]	$ET_o = 5.43u^{0.456}(e_s-e_a)$	T,T_{min}, T_{max},RH,u
Dalton	Dalton [27]	$ET_o = (3.648+0.7223u)(e_s-e_a)$	T,T_{min}, T_{max},RH,u
Ivanov	Romanenko [28]	$ET_o = 0.00006(25+T)^2(100-RH)$	T,RH
Mahringer	Mahringer [29]	$ET_o = 2.8597u^{0.5}(e_s-e_a)$	T,T_{min}, T_{max},RH,u
Meyer	Meyer [30]	$ET_o = (3.75+0.5026u)(e_s-e_a)$	T,T_{min}, T_{max},RH,u
Papadakis	Papadakis [31]	$ET_o = 2.5(e_{ma}-e_a)$	T_{min},T_{max},RH
Penman	Penman [32]	$ET_o = (2.625+0.000479/u)(e_s-e_a)$	T,T_{min}, T_{max},RH,u
Rohwer	Rohwer [33]	$ET_o = (3.3+0.891u)(e_s-e_a)$	T,T_{min}, T_{max},RH,u
Trabert	Trabert [34]	$ET_o = 3.075u^{0.5}(e_s-e_a)$	T,T_{min}, T_{max},RH,u
WMO	WMO [35]	$ET_o = (1.298+0.934u)(e_s-e_a)$	T,T_{min}, T_{max},RH,u

ET_o is the reference crop evapotranspiration (mm/day)

R_n is the net radiation (MJ/m^2/day)

G is the soil heat flux (MJ/m^2/day)

γ is the psychrometric constant (kPa/℃)

e_s is the saturation vapour pressure (kPa)

e_a is the actual vapour pressure (kPa)

Δ is the slope of the saturation vapour pressure–temperature curve (kPa/℃)

T is the average daily air temperature (℃)

u is the mean daily wind speed at 2 m (m/s)

H is the elevation (m), φ is the latitude (rad)

T_{min} is the minimum air temperature (℃)

T_{max} is the maximum air temperature (℃)

RH is the average relative humidity (%)

n is the actual duration of sunshine (hr)

R_s is the solar radiation (MJ/m^2/day)

e_{ma} is the saturation vapour pressure at the monthly mean daily maximum temperature (kPa)

Table 3 Error of model calculated for each province

	Al.	BW	Da.	Iv.	Ma.	Me.	Pa.	Pe.	Ro.	Tr.	WMO
CB	**0.9671**	0.9251	0.8806	0.8586	0.9319	0.8696	0.8192	0.839	0.8911	0.9319	0.9295
EA	0.9397	0.9567	0.9555	**0.9601**	0.9557	0.9571	0.9596	0.9575	0.9537	0.9557	0.9468
WA	**0.962**	0.94	0.9221	0.9167	0.9431	0.9168	0.8926	0.9012	0.9271	0.9431	0.9443
AR	0.9487	0.9601	0.9599	0.9568	0.9596	**0.9603**	0.9415	0.956	0.9592	0.9596	0.9547
ES	**0.978**	0.9424	0.9218	0.8907	0.9477	0.9096	0.8464	0.8663	0.9321	0.9477	0.9604
IL	**0.943**	0.9345	0.9295	0.9271	0.9358	0.9267	0.9222	0.9166	0.9318	0.9358	0.9382
BU	0.961	**0.9854**	0.9837	0.9684	0.9852	0.9802	0.8932	0.95	0.9849	0.9852	0.9783
TE	**0.9826**	0.9506	0.9403	0.9075	0.9551	0.9297	0.8969	0.8879	0.9488	0.9551	0.9702
AL	**0.9687**	0.9519	0.942	0.9164	0.9545	0.9357	0.9165	0.9115	0.9471	0.9545	0.9606
SK	0.9564	**0.9716**	0.9694	0.9453	0.9711	0.9689	0.9258	0.9576	0.9691	0.9711	0.9643
RK	0.9585	0.9597	0.9566	0.9473	**0.9601**	0.9552	0.941	0.9486	0.9576	**0.9601**	0.9592
NK	0.9479	0.9537	0.9491	0.9309	**0.9541**	0.9468	0.9289	0.9321	0.9505	**0.9541**	0.9512
KH	0.9683	0.9673	0.9634	0.9497	0.9684	0.9597	0.919	0.9399	0.9658	0.9684	**0.9695**
ZA	**0.945**	0.9333	0.9251	0.9163	0.935	0.9215	0.9066	0.9097	0.9282	0.935	0.9376
SE	**0.9553**	0.9447	0.9323	0.9337	0.9466	0.9285	0.9219	0.9161	0.9357	0.9466	0.9463
SB	0.9766	0.9692	0.9655	0.9228	0.9714	0.9589	0.8846	0.925	0.97	0.9714	**0.9775**
FA	**0.9681**	0.9439	0.9334	0.9138	0.9471	0.9262	0.8944	0.9001	0.9394	0.9471	0.9562
QO	**0.9595**	0.9498	0.9384	0.914	0.9519	0.9319	0.8929	0.9055	0.9433	0.9519	0.9549
GH	**0.9558**	0.9437	0.936	0.9253	0.9454	0.9321	0.9177	0.9183	0.9393	0.9454	0.9487

KO	**0.9388**	0.9209	0.9123	0.9094	0.9231	0.9081	0.8968	0.8946	0.9161	0.9231	0.928
KE	**0.9779**	0.9677	0.9636	0.9353	0.9696	0.9582	0.897	0.9309	0.9675	0.9696	0.9752
KS	**0.9438**	0.9287	0.9237	0.9136	0.9304	0.9202	0.9175	0.908	0.9268	0.9304	0.936
KB	**0.9178**	0.9059	0.8895	0.8758	0.9082	0.8849	0.8731	0.8707	0.8937	0.9082	0.907
GO	**0.9555**	0.9452	0.9229	0.9066	0.9475	0.9175	0.9007	0.9009	0.9277	0.9475	0.9432
GI	**0.971**	0.9683	0.9633	0.9689	0.9689	0.9622	0.9251	0.9592	0.9643	0.9689	0.9679
LO	**0.9234**	0.9059	0.8959	0.893	0.9081	0.8925	0.8869	0.8825	0.8991	0.9081	0.9106
MZ	**0.964**	0.9344	0.9178	0.9191	0.9383	0.9101	0.8617	0.8853	0.9245	0.9383	0.9459
MA	**0.9548**	0.9236	0.9003	0.8867	0.9279	0.8924	0.8632	0.8689	0.9074	0.9279	0.9317
HO	**0.9742**	0.9558	0.947	0.8083	0.959	0.9381	0.8165	0.8954	0.9535	0.959	0.9676
HA	**0.9687**	0.9292	0.9003	0.8767	0.9351	0.8893	0.834	0.8566	0.9101	0.9351	0.9425
YA	**0.9639**	0.9524	0.9468	0.9289	0.9542	0.942	0.912	0.9219	0.9505	0.9542	0.9594

Al. is Albrecht, BW is Brockamp-Wenner, Da. is Dalton, Iv. is Ivanov, Ma. is Mahringer, Me. is Meyer, Pa. is Papadakis, Pe. is Penman, Ro. is Rohwer, and Tr. is Trabert, the underlines show the best value of each method and the bolds show the best value of each province

Table 4 The best range to use the models based on the results of the current study

Model	T	T_{max}	T_{min}	RH	u	R^2
Albrecht	16-18	22.5-24.0	11-13	40-45	2.50-2.75	0.9826
Brockamp-Wenner	24-26	28.5-30	19-21	65-70	3.00-3.25	0.9854
Dalton	16-18	24.0-25.5	7-9	35-40	2.50-2.75	0.9694
Ivanov	14-16	–	–	>80	–	0.9689
Mahringer	24-26	28.5-30	19-21	65-70	3.00-3.25	0.9852
Meyer	24-26	28.5-30	19-21	65-70	3.00-3.25	0.9802
Papadakis	12-14	18.0-19.5	5-7	50-55	3.00-3.25	0.9596
Penman	14-16	19.5-21.0	11-13	>80	1.25-1.50	0.9592
Rohwer	18-20	25.5-27.0	9-11	<35	3.25-3.50	0.97
Trabert	24-26	28.5-30	19-21	65-70	3.00-3.25	0.9852
WMO	24-26	28.5-30	19-21	65-70	3.00-3.25	0.9783

T is the average daily air temperature (℃), u is the mean daily wind speed at 2 m (m/s), T_{min} is the minimum air temperature (℃), T_{max} is the maximum air temperature (℃), and RH is the average relative humidity (%)

Figure 1

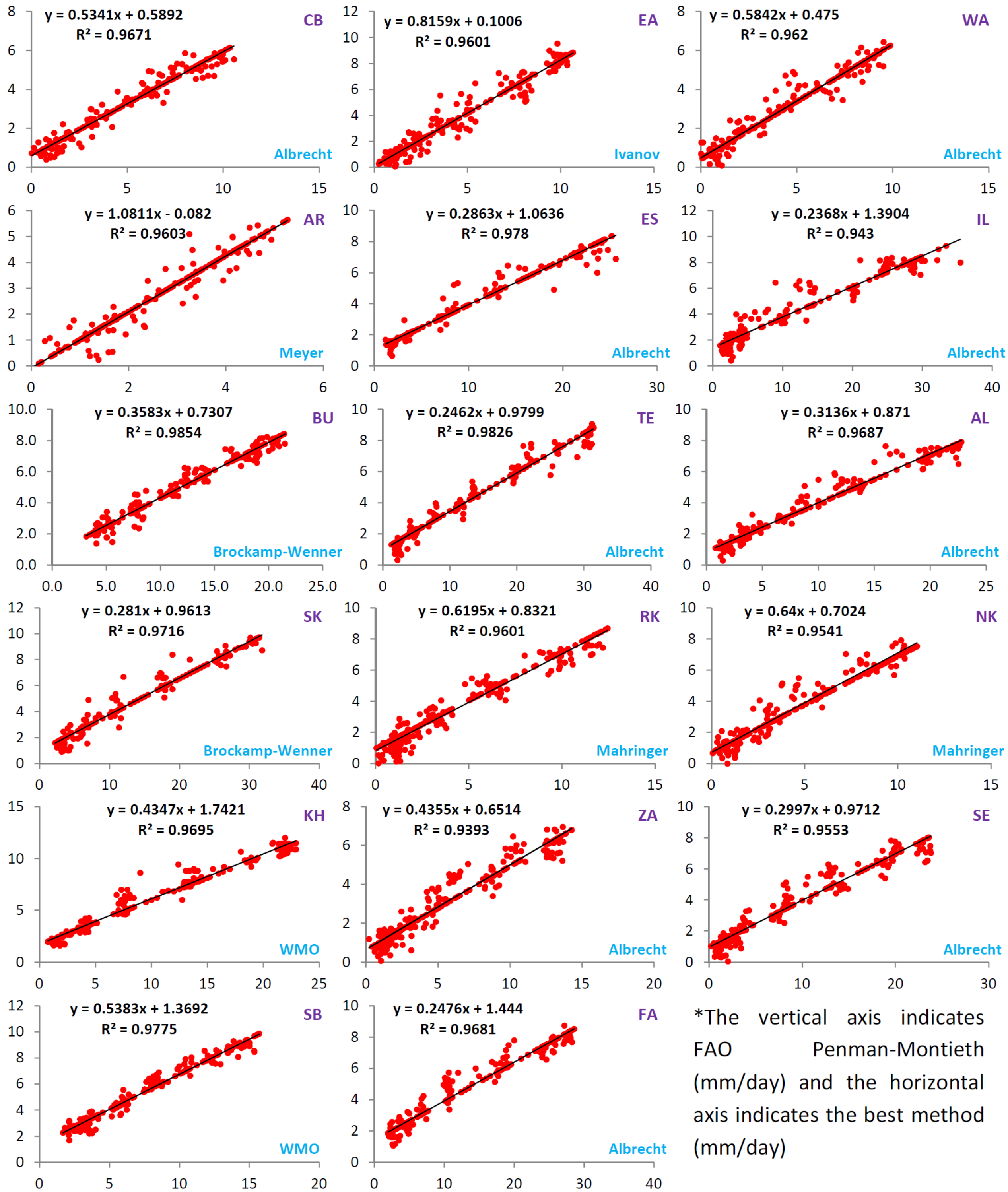

*The vertical axis indicates FAO Penman-Montieth (mm/day) and the horizontal axis indicates the best method (mm/day)

Figure 1 (continued)

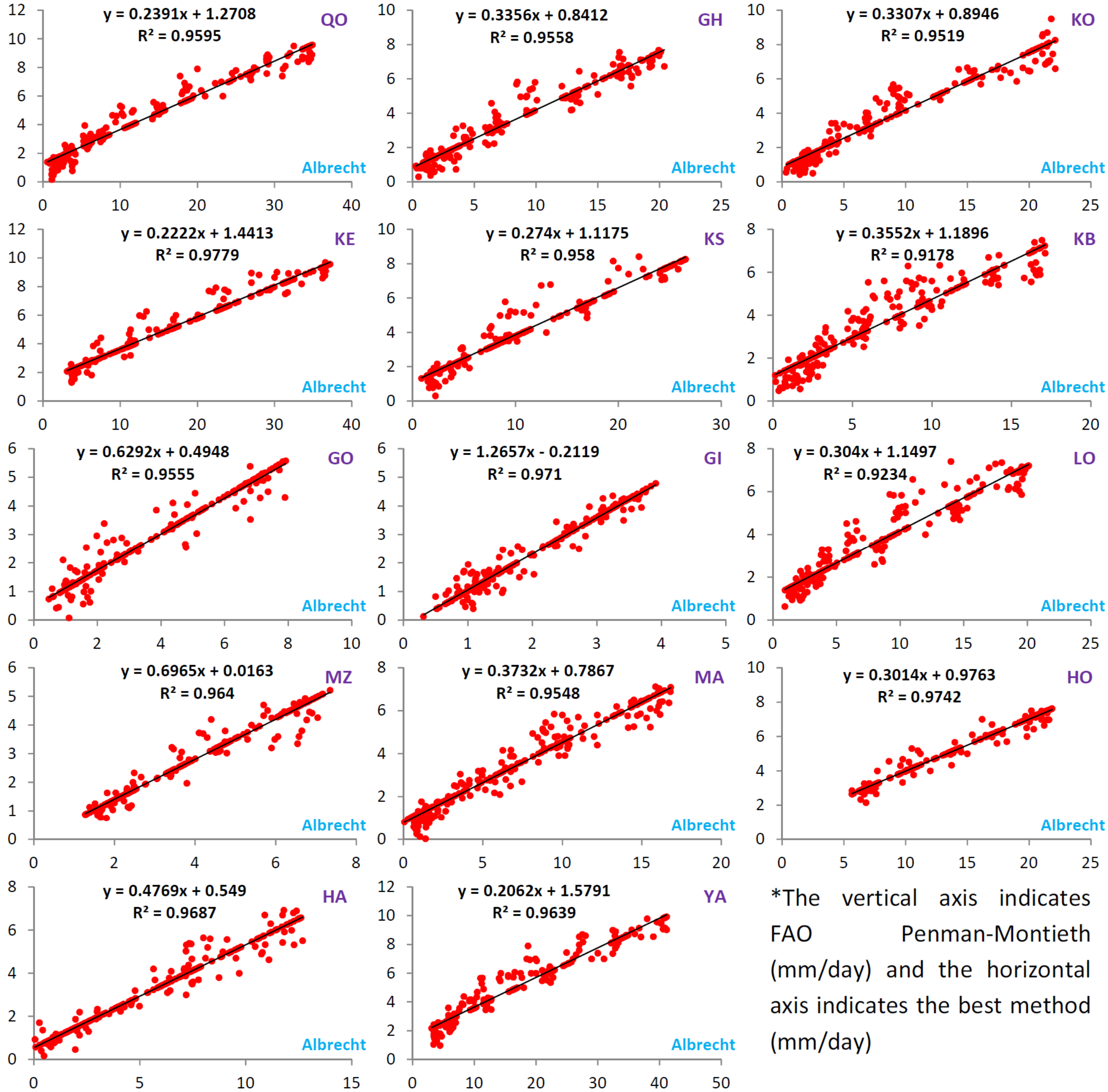

*The vertical axis indicates FAO Penman-Montieth (mm/day) and the horizontal axis indicates the best method (mm/day)

Figure 2

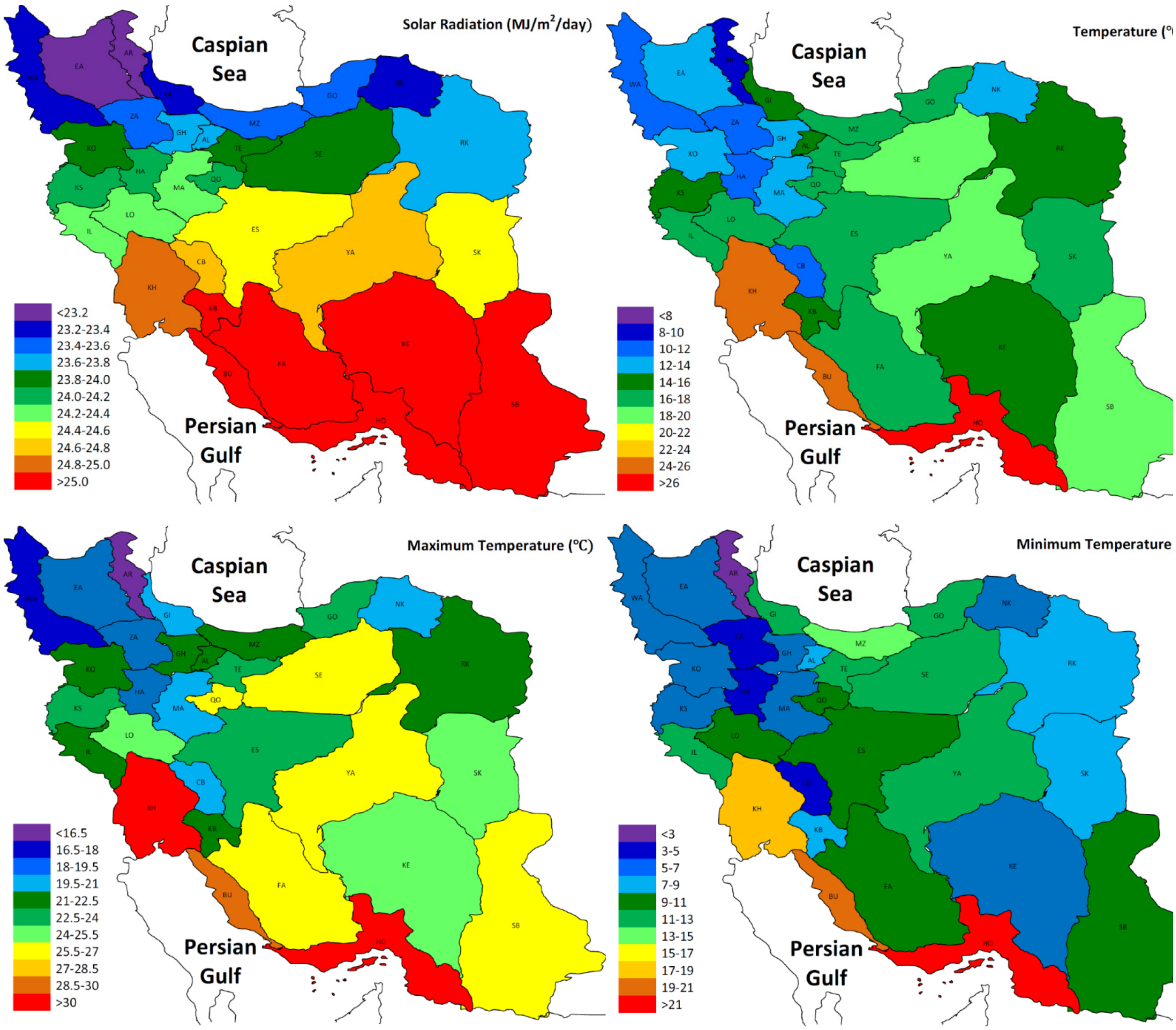
Caspian Sea
Solar Radiation (MJ/m²/day)
<23.2
23.2-23.4
23.4-23.6
23.6-23.8
23.8-24.0
24.0-24.2
24.2-24.4
24.4-24.6
24.6-24.8
24.8-25.0
>25.0
Persian Gulf
Caspian Sea
Temperature (°
<8
8-10
10-12
12-14
14-16
16-18
18-20
20-22
22-24
24-26
>26
Persian Gulf
Caspian Sea
Maximum Temperature (°C)
<16.5
16.5-18
18-19.5
19.5-21
21-22.5
22.5-24
24-25.5
25.5-27
27-28.5
28.5-30
>30
Persian Gulf
Caspian Sea
Minimum Temperature
<3
3-5
5-7
7-9
9-11
11-13
13-15
15-17
17-19
19-21
>21
Persian Gulf

Figure 3

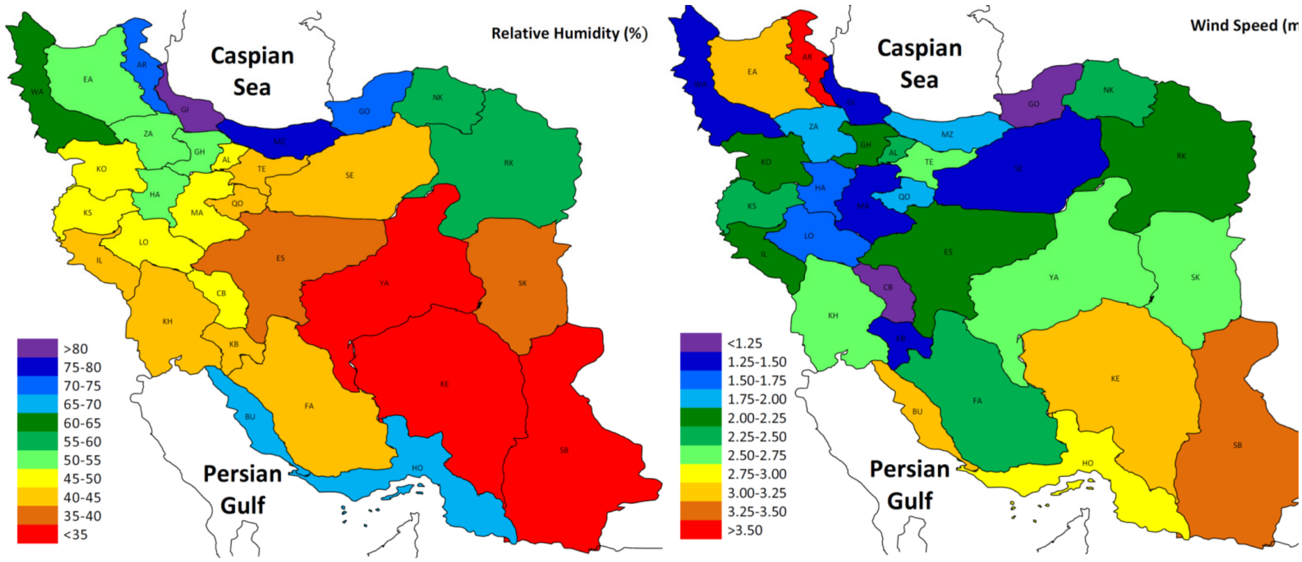
Relative Humidity (%)
Caspian Sea
Persian Gulf
>80
75-80
70-75
65-70
60-65
55-60
50-55
45-50
40-45
35-40
<35
Wind Speed (m
Caspian Sea
Persian Gulf
<1.25
1.25-1.50
1.50-1.75
1.75-2.00
2.00-2.25
2.25-2.50
2.50-2.75
2.75-3.00
3.00-3.25
3.25-3.50
>3.50

Figure 4

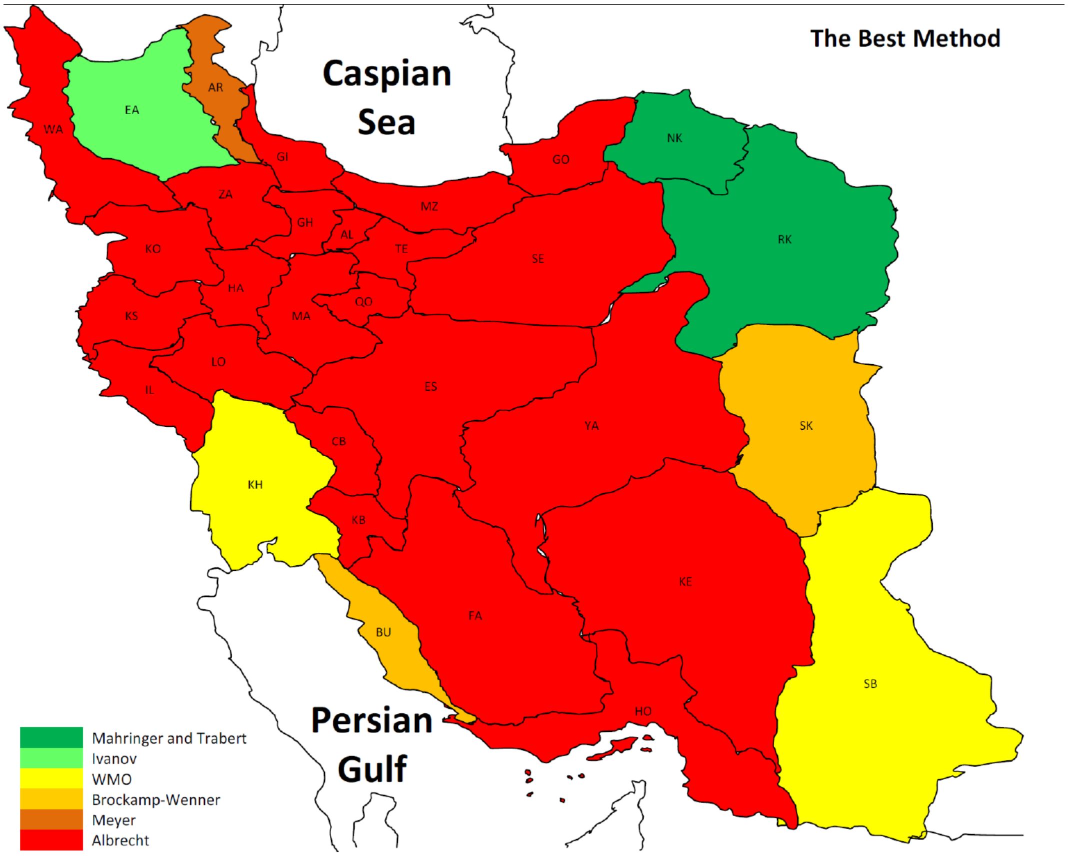
The Best Method
Caspian Sea
Persian Gulf
WA
EA
AR
GI
GO
NK
RK
ZA
MZ
GH
AL
TE
SE
KO
HA
QO
MA
KS
LO
IL
ES
YA
SK
CB
KH
KB
KE
FA
BU
SB
HO
Mahringer and Trabert
Ivanov
WMO
Brockamp-Wenner
Meyer
Albrecht

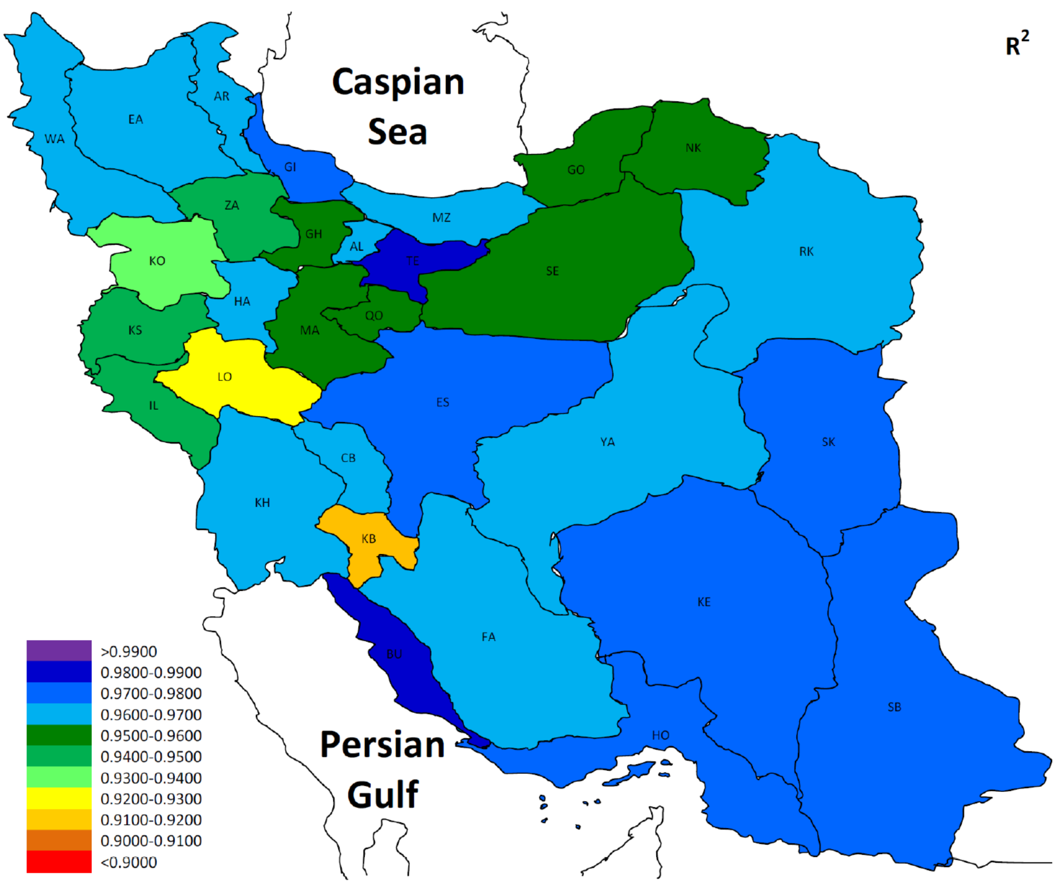
R^2
Caspian Sea
Persian Gulf
WA
EA
AR
GI
GO
NK
ZA
MZ
GH
AL
TE
RK
KO
SE
HA
QO
KS
MA
LO
ES
IL
YA
SK
CB
KH
KB
KE
FA
BU
SB
HO
>0.9900
0.9800-0.9900
0.9700-0.9800
0.9600-0.9700
0.9500-0.9600
0.9400-0.9500
0.9300-0.9400
0.9200-0.9300
0.9100-0.9200
0.9000-0.9100
<0.9000

References

[1] Anctil, F., C., Perrin and V., Andre´assian, 2004. Impact of the length of observed records on the performance of ANN and of conceptual parsimonious rainfall-runoff forecasting models, Environmental Modeling & Software, 19, pp: 357–368. DOI: 10.1016/S1364-8152(03)00135-X

[2] Andrieu, H., M. N., French, V., Thauvin and V. F., V., Krajewski, 1996. Adaptation and application of a quantitative rainfall forecasting model in a mountainous region, Journal of Hydrology, 184(3-4), pp: 243–259. DOI: http://dx.doi.org/10.1016/0022-1694(95)02977-X

[3] Balaguer, E., A. Palomares, E. Sorie and J.D. Martin-Guerrero, 2008. Predicting service request in support centers based on nonlinear dynamics, ARMA modeling and neural networks. Expert Systems with Applications, 34(1), pp: 665–672. DOI: 10.1016/j.eswa.2006.10.003

[4] Box, G.E.P., G.M., Jenkins, 1976. Series Analysis Forecasting and Control. Prentice-Hall Inc., London.

[5] Burlando, C., R., Rosso, L. G., Cadavid and J. D., Salas, 1993. Forecasting of short-term rainfall using ARMA models, Journal of Hydrology, 144(1-4), pp: 193–211. DOI: http://dx.doi.org/10.1016/0022-1694(93)90172-6

[6] Chattopadhyay, S. and G., Chattopadhyay, 2010. Univariate modelling of summer-monsoon rainfall time series: Comparison between ARIMA and ARNN, Comptes Rendus Geoscience, 342(2), pp: 100–107. DOI: http://dx.doi.org/10.1016/j.crte.2009.10.016

[7] Chenoweth, T., K. Dowling, R., Hubata and R. Louis, 2004. Automatic ARMA identification using neural networks and the extended sample autocorrelation function: a reevaluation. Decision Support Systems, 29, pp: 21-30. DOI: http://dx.doi.org/10.1016/S0167-9236(00)00058-0

[8] Chenoweth, T., K. Dowling, R., Hubata, and R. Louis, 2004. Distance and prediction error variance constraints for ARMA model portfolios. International Journal of Forecasting, 20, pp: 41-52. DOI: http://dx.doi.org/10.1016/S0169-2070(03)00006-2

[9] Han, P., P.X., Wang, S. Y., Zhang and D. H. Zhu, 2010. Drought forecasting based on the remote sensing data using ARIMA models, Mathematical and Computer Modelling, 51(11-12), pp: 1398–1403. DOI: http://dx.doi.org/10.1016/j.mcm.2009.10.031

[10] Hu, W., S., Tong, K., Mengersen and B., Oldenburg, 2006. Rainfall, mosquito density and the transmission of Ross River virus: A time-series forecasting model, 196(3-4), pp: 505–514. DOI: http://dx.doi.org/10.1016/j.ecolmodel.2006.02.028

[11] Jia, Y. and Culver T. B., 2006. Bootstrapped artificial neural networks for synthetic flow generation with a small data sample, Journal of Hydrology, 331, pp: 580– 590. DOI: 10.1016/j.jhydrol.2006.06.005

[12] Karamouz, M., Araghinejad Sh., 2012. Advance Hydrology, Amirkabir University of Technology Press.

[13] Luc, K. C., J. e., Ball and A., Sharma, 2001. An application of artificial neural networks for rainfall forecasting, Mathematical and Computer Modelling, 33(6-7), pp: 683–693. DOI: http://dx.doi.org/10.1016/S0895-7177(00)00272-7

[14] Ludlow, J. and W. Enders, 2000. Estimating non-linear ARMA models using Fourier Coefficients, International Journal of Forecasting, 16(3), pp: 333-347.

[15] M. Baareh, A.K., A. F. Sheta and Kh. Al Khnaifes, 2006, Forecasting River Flow in the USA: A Comparison between Auto-Regression and Neural Network Non-Parametric Models, Journal of Computer Science, 2 (10), pp: 775-780.

[16] Mohammadi, K., H.R. Eslami and S. Dayyani Dardashti, 2005. Comparison of Regression ARIMA and ANN Models for Reservoir Inflow Forecasting using Snowmelt Equivalent (A Case Study of Karaj), Journal of Agriculture Science Technology, 7, pp. 17-30.

[17] Mohammadi, K., H.R. Eslami and R. Kahawita, 2006. Parameter estimation of an ARMA model for river flow forecasting using goal programmin, Journal of Hydrology, 331 (2), pp: 293–299, DOI: 10.1016/j.jhydrol.2006.05.017

[18] Ramírez, M. C. V., H. F. D. C., Velho and N. J. Ferreira, 2005. Artificial neural network technique for rainfall forecasting applied to the São Paulo region, Journal of Hydrology, 301(1-4), pp: 146–162. DOI: http://dx.doi.org/10.1016/j.jhydrol.2004.06.028

[19] See, L., and R.J. Abrahat, 2001. Multi-model data fusion for hydrological forecasting, Computers & Geosciences, 27, pp: 987–994, DOI: http://dx.doi.org/10.1016/S0098-3004(00)00136-9

[20] Serinaldi, F. and C. G., Kilsb, 2012. A modular class of multisite monthly rainfall generators for water resource management and impact studies, Journal of Hydrology, DOI: http://dx.doi.org/10.1016/j.jhydrol.2012.07.043

[21] Srinivas, V.V., and K. Srinivasan, 2000. Post-blackening approach for modeling dependent annual streamflows, Journal of Hydrology, 230, pp: 86–126, DOI: http://dx.doi.org/10.1016/S0022-1694(00)00168-2

[22] Toth, E., A. Brath, and A. Montanari, 2000. Comparison of short-term rainfall predication models for real-time flood forecasting, Journal of Hydrology, 239, pp: 132–147, DOI: http://dx.doi.org/10.1016/S0022-1694(00)00344-9

[23] Rezaei, M., Valipour, M., Valipur, M. 2016. Modelling evapotranspiration to increase the accuracy of the estimations based on the climatic parameters. Water Conservation Science and Engineering. In Press.

[24] Wei, C., W. C., Hung and K. S., Cheng, 2006. A multi-spectral spatial convolution approach of rainfall forecasting using weather satellite imagery, Advances in Space Research, 37(4), pp: 747–753. DOI: http://dx.doi.org/10.1016/j.asr.2005.08.017

[25] Xiong, L. and K. M. O'connor, 2002, Comparison of four updating models for real-time river flow forecasting, Hydrological Sciences-Journal-des Sciences Hydrologiques, 47(4), pp: 621-639.

[26] Yu, X., and S. Liong, 2006. Forecasting of hydrologic time series with ridge regression in feature space, Journal of Hydrology, 332, pp: 290– 302, DOI: http://dx.doi.org/10.1016/j.jhydrol.2006.07.003

[27] Khoshravesh, M., Gholami Sefidkouhi, M.A., Valipour, M., 2015. Estimation of reference evapotranspiration using multivariate fractional polynomial, Bayesian regression, and robust regression models in three arid environments. In Press. Applied Water Science. http://dx.doi.org/10.1007/s13201-015-0368-x

[28] Valipour, M., Singh, V.P., 2016. Global Experiences on Wastewater Irrigation: Challenges and Prospects. Balanced Urban Development: Options and Strategies for Liveable Cities. Basant Maheshwari, Vijay P. Singh, Bhadranie Thoradeniya, (Eds.). AG: Springer. Switzerland. 289-327.

[29] Valipour, M., Gholami Sefidkouhi, M.A., Raeini-Sarjaz, M., 2017a. Selecting the best model to estimate potential evapotranspiration with respect to climate change and magnitudes of extreme events. Agricultural Water Management. In Press. http://dx.doi.org/10.1016/j.agwat.2016.08.025

[30] Valipour, M., Gholami Sefidkouhi, M.A., Khoshravesh, M., 2017b. Estimation and trend evaluation of reference evapotranspiration in a humid region. Italian Journal of Agrometeorology. In Press.

[31] Valipour, M., 2015a. Future of agricultural water management in Africa. Archives of Agronomy and Soil Science. 61 (7), 907-927.

[32] Valipour, M., 2015b. Calibration of mass transfer-based models to predict reference crop evapotranspiration. Applied Water Science. In Press. http://dx.doi.org/10.1007/s13201-015-0274-2

[33] Valipour, M., 2015c. Analysis of potential evapotranspiration using limited weather data. Applied Water Science. In Press. http://dx.doi.org/10.1007/s13201-014-0234-2

[34] Valipour, M., 2015d. Handbook of Environmental Engineering Problems. Foster City, CA: OMICS Press. USA. http://esciencecentral.org/ebooks/handbook-of-environmental-engineering-problems/

[35] Valipour, M., 2013a. INCREASING IRRIGATION EFFICIENCY BY MANAGEMENT STRATEGIES: CUTBACK AND SURGE IRRIGATION. ARPN J. Agricultural and Biological Science. 8 (1), 35-43.

[36] Valipour, M., 2013b. Necessity of Irrigated and Rainfed Agriculture in the World. Irrigation & Drainage Systems Engineering. S9, e001. http://omicsgroup.org/journals/necessity-of-irrigated-and-rainfed-agriculture-in-the-world-2168-9768.S9-e001.php?aid=12800

[37] Valipour, M., 2013c. Evolution of Irrigation-Equipped Areas as Share of Cultivated Areas. Irrigation & Drainage Systems Engineering. 2 (1), e114. http://dx.doi.org/10.4172/2168-9768.1000e114

[38] Valipour, M., 2013d. USE OF SURFACE WATER SUPPLY INDEX TO ASSESSING OF WATER RESOURCES MANAGEMENT IN COLORADO AND OREGON, US. Advances in Agriculture, Sciences and Engineering Research. 3 (2), 631-640. http://vali-pour.webs.com/13.pdf

[39] Valipour, M., 2012a. HYDRO-MODULE DETERMINATION FOR VANAEI VILLAGE IN ESLAM ABAD GHARB, IRAN. ARPN Journal of Agricultural and Biological Science. 7 (12), 968-976.

[40] Valipour, M., 2012b. Ability of Box-Jenkins Models to Estimate of Reference Potential Evapotranspiration (A Case Study: Mehrabad Synoptic Station, Tehran, Iran). IOSR Journal of Agriculture and Veterinary Science (IOSR-JAVS). 1 (5), 1-11. http://dx.doi.org/10.9790/2380-0150111

[41] Valipour, M., 2012c. A Comparison between Horizontal and Vertical Drainage Systems (Include Pipe Drainage, Open Ditch Drainage, and Pumped Wells) in Anisotropic Soils. IOSR Journal of Mechanical and Civil Engineering (IOSR-JMCE). 4 (1), 7-12. http://dx.doi.org/10.9790/1684-0410712
[42] Valipour, M., 2014. Application of new mass transfer formulae for computation of evapotranspiration. Journal of Applied Water Engineering and Research. 2 (1), 33-46.